Electronic Supplementary Material (ESI) for Chemical Communications

Supporting Information

for

Pyridine-2-thiolate bridged tin-palladium-complexes with $Sn(PdN_2Cl_2)$, $Sn(PdN_2S_2)$, $Sn(PdN_2C_2)$ and $Sn(Pd_2N_4)$ skeleton

Erik Wächtler, Robert Gericke, Lyuben Zhechkov, Thomas Heine, Thorsten Langer, Birgit Gerke, Rainer Pöttgen and Jörg Wagler*

Experimental section:

General considerations:

All reactions were carried out under an atmosphere of dry argon using standard Schlenk techniques. The solvents and triethylamine were dried according to standard methods (THF, diethyl ether and triethylamine: distillation from Na/benzophenone; toluene, pentane: distillation from Na; chloroform, dimethyl sulfoxide: storage over molecular sieves 3Å). $Sn(PyS)_2$ (**III**),[1] $Sn(PyS)_2Cl_2$ (**IV**),[2] $Sn(PyS)_4$ (**V**),[1] $Sn(PyS)_2Ph_2$ (**VI**),[3] $[Pd(PyS)_2(PPh_3)_2]$[4], $SnCl_2$(dioxane)[5] and $[PdCl_2(PPh_3)_2]$[6] were prepared following literature methods; all other chemicals were commercially available and used as received. A "Polytherm A" microscope with heating function (Wagner&Munz, Munich, Germany) was used for the determination of the melting points; they are not corrected. Elemental analyses were carried out with a "Vario Micro Cube" analyser (Elementar, Hanau, Germany). ^{1}H, ^{13}C, ^{31}P and ^{119}Sn NMR spectra were recorded on a "Bruker DPX 400" spectrometer or on a "Bruker AVANCE 500" spectrometer in $CDCl_3$, D6-DMSO or CD_2Cl_2. Chemical shifts are given in ppm. The spectra are referenced against internal $SiMe_4$ (^{1}H, ^{13}C), external 85% H_3PO_4 (^{31}P) or external $SnMe_4$ (^{119}Sn). ^{119}Sn MAS NMR spectra were recorded on a "Bruker Avance 400 WB" spectrometer (using a 4 mm ZrO_2 spinner) and referenced against external SnO_2 (-603 ppm). Single-crystal X-ray diffraction data were collected on a Stoe IPDS-2/2T diffractometer using graphite monochromated Mo-Kα radiation (λ = 0.71073 Å). Crystals were selected under an inert oil and mounted on a glass capillary which was coated with a thin layer of silicone grease. The structures were solved by direct methods using SHELXS-97 and refined anisotropically against $|F^2|$ in a full-matrix lesast-squares refinement with the SHELXL-97 program.[7] Hydrogen atoms were refined isotropically in idealized positions (riding model). ^{119}Sn Mössbauer spectra were recorded at 78 K with a $CaSnO_3$ source.

Syntheses of compound 1:

Route A: synthesis out of $Sn(PyS)_2$ (**III**) and $[PdCl_2(PPh_3)_2]$

At room temperature solid $[PdCl_2(PPh_3)_2]$ (100 mg, 136 µmol) was added to a stirred solution of $Sn(PyS)_2$ (46 mg, 136 µmol) in THF (1 mL). The colour of the solution changed immediately to red. After slow vapour diffusion of diethyl ether into the solution (over a period of 5 d), 79 mg (101 µmol, 78%) of the product **1** were obtained as red crystals, which were separated by decantation, washed with a mixture of THF/diethyl ether (1:1, 1 mL) and dried in vacuo.

Route B: synthesis out of $Sn(PyS)_2Cl_2$ (**IV**) and $[Pd(PPh_3)_4]$

At room temperature $[Pd(PPh_3)_4]$ (400 mg, 346 µmol) was stirred in THF (3 mL) and solid $Sn(PyS)_2Cl_2$ (**IV**) (148 mg, 346 µmol) was added, whereupon the reactants dissolved to afford a red solution. Vapour diffusion of diethyl ether into the solution afforded compound **1** as red crystals, which were separated by decantation after 5 d, washed with a THF/diethyl ether mixture (1:1, 1 mL) and dried under vacuum. Yield: 212 mg (273 µmol, 79%).

Route C: synthesis out of $SnCl_2$(dioxane) and $[Pd(PyS)_2(PPh_3)_2]$

At room temperature $[Pd(PyS)_2(PPh_3)_2]$ (60 mg, 71 µmol) was stirred in THF (2 mL) and solid $SnCl_2$(dioxane) (20 mg, 71 µmol) was added, whereupon a red solution formed. Vapour diffusion of diethyl ether into this solution afforded red crystals after a few days. The supernatant was decanted off and the product was washed with a THF/diethyl ether mixture (1:1, 1 mL) and briefly dried under vacuum. Yield: 41 mg (53 µmol, 75%).

Route D: synthesis out of $[PdCl(SnCl_3)(PPh_3)_2]$ (**2**)

At room temperature $[PdCl(SnCl_3)(PPh_3)_2]$ (63 mg, 56 µmol) and H(PyS) (13 mg, 115 µmol) were stirred in THF (3 mL). Upon addition of triethylamine (21 µl, 150 µmol) via mycro syringe and stirring for a few hours the initially yellow suspension turned into a red solution and a colourless precipitate (of Et_3NHCl). Thereafter, the mixture was filtered and diethyl ether was allowed to enter the filtrate by slow vapour diffusion to afford 11 mg (14 µmol, 25%) of the red crystalline product.

Analyses for compound **1**:

m.p. not observed (decomposition >280°C)

C/H/N/S microanalysis calcd (%) for $C_{28}H_{23}Cl_2N_2PPdS_2Sn$: C 43.19, H 2.98, N 3.60, S 8.23; found: C 42.92, H 3.01, N 3.49, S 8.16

^{1}H NMR ($CDCl_3$): δ 7.04 (m, 2H, N-CH-C*H*), 7.39 (m, 2H, N-CH-CH-C*H*), 7.56 (d, $^3J(^1H\text{-}^1H)$=8.0 Hz, 2H, N-CH-CH-CH-C*H*), 8.59 (d, $^3J(^1H\text{-}^1H)$=5.4 Hz, 2H, N-C*H*), 7.43-7.53 (mm, 9H, Ph), 7.60-7.72 (m, 6H, Ph)

$^{13}C\{^1H\}$ NMR ($CDCl_3$): δ 118.2 (*C*-5, PyS), 125.2 (*C*-3, PyS), 128.4 (d, $^3J(^{13}C\text{-}^{31}P)$=11 Hz, Ph_{meta}), 129.6 (d, $^1J(^{13}C\text{-}^{31}P)$=41 Hz, Ph_{ipso}), 130.9 (Ph_{para}), 134.7 (d, $^2J(^{13}C\text{-}^{31}P)$=12 Hz, Ph_{ortho}), 137.7 (*C*-6, PyS), 145.5 (*C*-4, PyS), 158.2 (*C*-2, PyS)

$^{31}P\{^1H\}$ NMR ($CDCl_3$): δ 26.3 (satellites: d, $^2J(^{31}P\text{-}^{119/117}Sn)$: 4311 Hz and 4125 Hz)

$^{119}Sn\{^1H\}$ NMR ($CDCl_3$): δ -121.6 (d, $^2J(^{119}Sn\text{-}^{31}P)$ = 4315 Hz)

^{119}Sn MAS NMR: δ_{iso} -108.8

^{119}Sn Mössbauer: IS = 1.63(1) mm/s; QS = 1.67(1) mm/s

Crystallisation of compound **1** along the above synthesis procedures, i.e., vapour diffusion of diethyl ether into a THF solution of **1**, gave rise to crystals of "modification a" (Table SI2). In further experiments we encountered different crystalline varieties of 1, i.e., "modification b" of compound **1** was obtained by slow evaporation of a dichloromethane/ethanol solution of **1** at room temperature, and crystals of the chloroform solvate $\mathbf{1}\cdot(CHCl_3)_2$ were obtained from a chloroform solution of **1** at 6°C.

Synthesis of compound 2:

In a Schlenk tube $SnCl_2$(dioxane) (112 mg, 403µmol) and $[PdCl_2(PPh_3)_2]$ (300 mg, 403 µmol) were layered with chloroform (10 mL). Yellow crystals formed upon storage for about one week. The solution was removed by decantation and the crude product was washed with chloroform (2 mL) to remove remaining starting materials. After drying briefly under vacuum 257 mg (227 µmol, 56%) of compound **2** were obtained.

C/H microanalysis calcd (%) for $C_{36}H_{30}Cl_4P_2PdSn \cdot 2CHCl_3$: C 40.38, H 2.85; found: C 38.17, H 2.74. Traces of residual $[PdCl_2(PPh_3)_2]$ or loss of chloroform after sample preparation (or a combination of both) could account for the somewhat lower C and H contents found.

This compound appears to be insoluble in common organic solvents (such as chloroform, THF, toluene, dichloromethane, DMSO), therefore solution NMR data (neither ^{1}H nor ^{31}P) had not been obtained.

Synthesis of compound 3:

At room temperature a suspension of $[Pd(PPh_3)_4]$ (655 mg, 0.57 mmol) in THF (8.5 mL) was slowly added to a stirred solution of of $Sn(PyS)_4$ (**V**) (317 mg, 0.57 mmol) in THF (8.5 mL), whereupon a red solution was obtained. Slow vapour diffusion of diethyl ether into this solution afforded the product as orange crystals. After 6 d, the product was isolated by decantation, washed with diethyl ether (2 mL) and dried *in vacuo*. Yield: 385 mg (0.41 mmol, 73%). The product crystallises as THF solvate $Ph_3PPd(\mu\text{-}PyS)_2Sn(PyS)_2 \cdot THF$, as found by single-crystal X-ray diffraction analysis. This solvent of crystallisation was removed by drying in vacuo, and the results of the microanalysis are consistent with the values calculated for the solvent free form of compound **3**, thus the yield reported is based on the molar mass without solvent. This compound has only poor solubility in common organic solvents.

C/H/N/S microanalysis calcd (%) for $C_{38}H_{31}N_4PPdS_4Sn$: C 49.18, H 3.37, N 6.04, S 13,82; found: C 49.27, H 3.39, N 5.93, S 13.70

^{1}H NMR ($(D_3C)_2SO$): δ 6.93 (m, 2H, Aryl), 7.04-7.70 (m, 20H, Aryl)

$^{31}P\{^{1}H\}$ NMR ($(D_3C)_2SO$): δ 25.8 (satellites: d, $^{2}J(^{31}P\text{-}^{119/117}Sn)$: 4598 Hz and 4351 Hz)

^{119}Sn Mössbauer: IS = 2.05(1); QS = 3.27(1)

Synthesis of compound 4:

To a mixture of solid $Sn(PyS)_2Ph_2$ (**VI**) (218 mg, 0.44 mmol) and solid $[Pd(PPh_3)_4]$ (510 mg, 0.44 mmol) THF (4 mL) was added and the suspension was stirred while it was slightly warmed (40-50°C) to afford a clear solution. After cooling to room temperature, diethyl ether was allowed to slowly enter the solution (vapour diffusion). Yellow crystals formed within a few days, which were isolated by decantation, washed with a mixture of THF/diethyl ether (1:1, 1 mL) and dried *in vacuo*. Yield: 290 mg (0.34 mmol, 76%).

m.p. not observed (decomposition 220°C)

C/H/N/S microanalysis calcd (%) for $C_{40}H_{33}N_2PPdS_2Sn$: C 55.74, H 3.86, N 3.25, S 7.44; found: C 55.88, H 3.86, N 3.18, S 7.47

^{1}H NMR ($CDCl_3$): δ 6.54 (m, 2H, N-CH-C*H*), 7.10 (m, 2H, N-CH-CH-C*H*), 7.36 (d, $^{3}J(^{1}H\text{-}^{1}H)$=8.3 Hz, 2H, N-CH-CH-CH-C*H*), 7.23-7.29 (m, 6H, Ph), 7.42 (m, 12H, Ph), 7.65 (d, $^{3}J(^{1}H\text{-}^{1}H)$ = 5.0 Hz, 2H, N-C*H*), 7.69-7.74 (m, 7H, Ph)

$^{13}C\{^{1}H\}$ NMR ($CDCl_3$): δ 116.5 (*C*-5, PyS), 126.2 (*C*-3, PyS), 127.9 (Sn-Ph_{para}), 128.2 (d, $^{3}J(^{13}C\text{-}^{31}P)$=9 Hz, P-$Ph_{meta}$) 128.2 (s, P-$Ph_{para}$), 129.9 (Sn-$Ph_{meta}$), 131.7 (d, $^{1}J(^{13}C\text{-}^{31}P)$ = 35 Hz, P-Ph_{ipso}), 134.8 (d, $^{2}J(^{13}C\text{-}^{31}P)$ = 12 Hz, P-Ph_{ortho}), 135.8 (*C*-6, PyS), 136.1 (Sn-Ph_{ortho}), 145.4 (*C*-4, PyS), 150.0 (Sn-Ph_{ipso}), 165.2 (*C*-2, PyS)

$^{31}P\{^{1}H\}$ NMR ($CDCl_3$): δ 22.3 (satellites: d, $^{2}J(^{31}P\text{-}^{119/117}Sn)$ = 2677 Hz and 2550 Hz)

$^{119}Sn\{^{1}H\}$ NMR ($CDCl_3$): δ 1.4 (d, $^{2}J(^{119}Sn\text{-}^{31}P)$ = 2677 Hz)

^{119}Sn Mössbauer: IS = 1.54(1); QS = 2.86(1)

Synthesis of compound 5:

At room temperature THF (52 mL) was added to a mixture of solid $Sn(PyS)_4$ (**V**) (103 mg, 0.18 mmol) and solid $[Pd(PPh_3)_4]$ (536 mg, 0.46 mmol). The suspension was stirred for about 10 s to afford a red solution, whereupon stirring was stopped and the solution was stored undisturbed. The product crystallised within one day (orange crystals), whereupon the supernatant was decanted off and the solid was washed with THF (2 mL) and dried under vacuum. Yield: 197 mg (0.14 mmol, 77%). As shown by single-crystal X-ray diffraction, compound **5** crystallises as the THF solvate $Ph_3PPd(\mu\text{-}PyS)_2Sn(\mu\text{-}PyS)_2PdPPh_3 \cdot 2(THF)$. The results of the microanalysis are consistent with a composition of one THF molecule per molecule of **5**, thus it appears that one of the two THF molecules is lost upon drying. The yield reported is therefore based on the composition **5**·THF.

C/H/N/S microanalysis calcd (%) for $C_{60}H_{54}N_4OP_2Pd_2S_4Sn$: C 52.65, H 3.98, N 4,09, S 9.37; found: C 52.55, H 4.25, N 3.84, S 9.31

^1H NMR (CD_2Cl_2): δ 6.65 (m, 4H, Aryl), 7.19 (m, 4H, Aryl), 7.26-7.54 (m, 24H, Aryl), 7.63-7.70 (m, 10H, Aryl) 9.04 (d, $^3J(^1H\text{-}^1H)$=5.4 Hz, 4H, Aryl)

$^{31}P\{^1H\}$ NMR (CD_2Cl_2): δ 23.9

^{31}P CP/MAS NMR: δ 27.2 (s, satellites: d, $^2J(^{31}P\text{-}^{119/117}Sn)$: 2884 Hz, $^{119/117}Sn$ not resolved)

^{119}Sn Mössbauer spectroscopy:

A $Ca^{119m}SnO_3$ source was available for the ^{119}Sn Mössbauer spectroscopic investigation. The sample was placed within a PMMA container (2 cm diameter) at a thickness of about 10 mg Sn/cm^2 (if necessary, the sample was diluted with quartz powder). A palladium foil of 0.05 mm thickness was used to reduce the tin K X-rays concurrently emitted by this source. The measurement was conducted in the usual transmission geometry at 78 K. Fitting of the spectra was performed with the Normos-90 program system.[8] In addition to the spectra of compounds **1**, **3**, **4** and **5** (Figures SI1-SI4) we have recorded the ^{119}Sn Mössbauer spectrum of starting material **III** ($Sn(PyS)_2$) (Figure SI5) and have confirmed the ^{119}Sn Mössbauer literature data reported for starting materials **IV** ($Sn(PyS)_2Cl_2$) and **V** ($Sn(PyS)_4$).

Table SI1: ^{119}Sn Mössbauer fitting parameters for compounds **1**, **3**·(THF), **4**, **5**·$(THF)_2$ and **III**. (For compound **III** the fit was constrained to the same signal area for the two sites, and the line widths were kept fixed to the values reported in the table.)

compound	δ (mm s^{-1})	ΔEQ (mm s^{-1})	Γ (mm s^{-1})	Signal area
1	1.63(1)	1.67(1)	0.88(2)	100%
3·(THF)	1.81(1)	2.00(1)	1.05(1)	100%
4	1.54(1)	2.86(1)	0.85(1)	100%
5·$(THF)_2$	2.05(1)	3.27(1)	0.85(1)	100%
III	3.17(1)	1.91(1)	0.85	39%
	3.15(1)	1.23(1)	0.85	39%
	0.35(1)	0.72(2)	0.9	22%

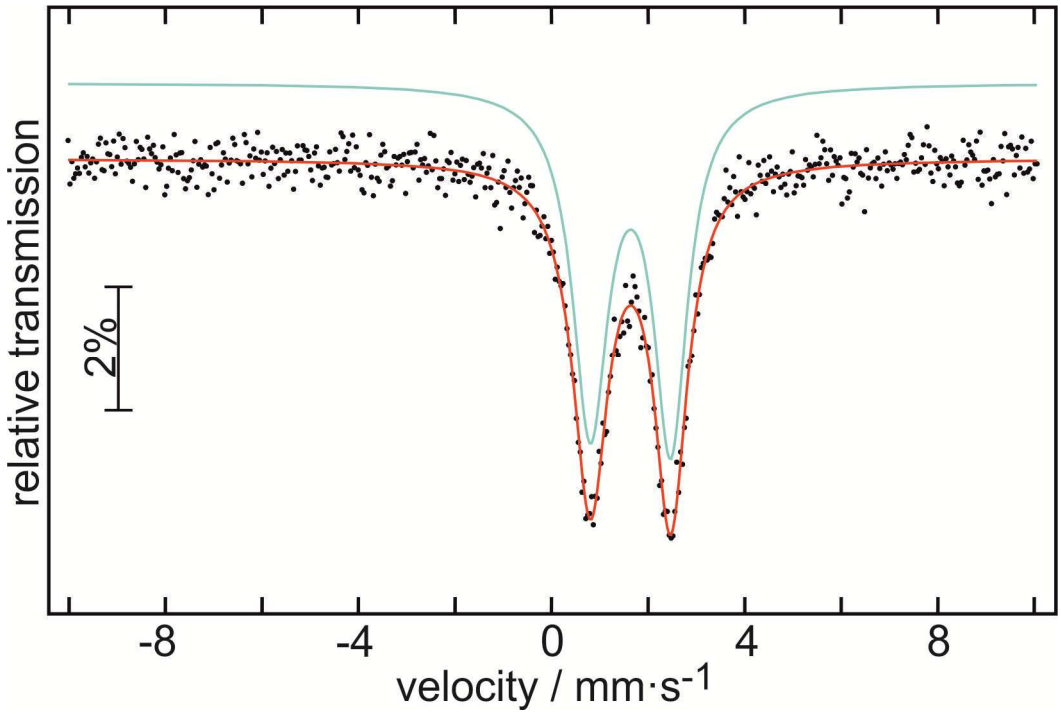

Figure SI1: ^{119}Sn Mössbauer spectrum of compound **1**.

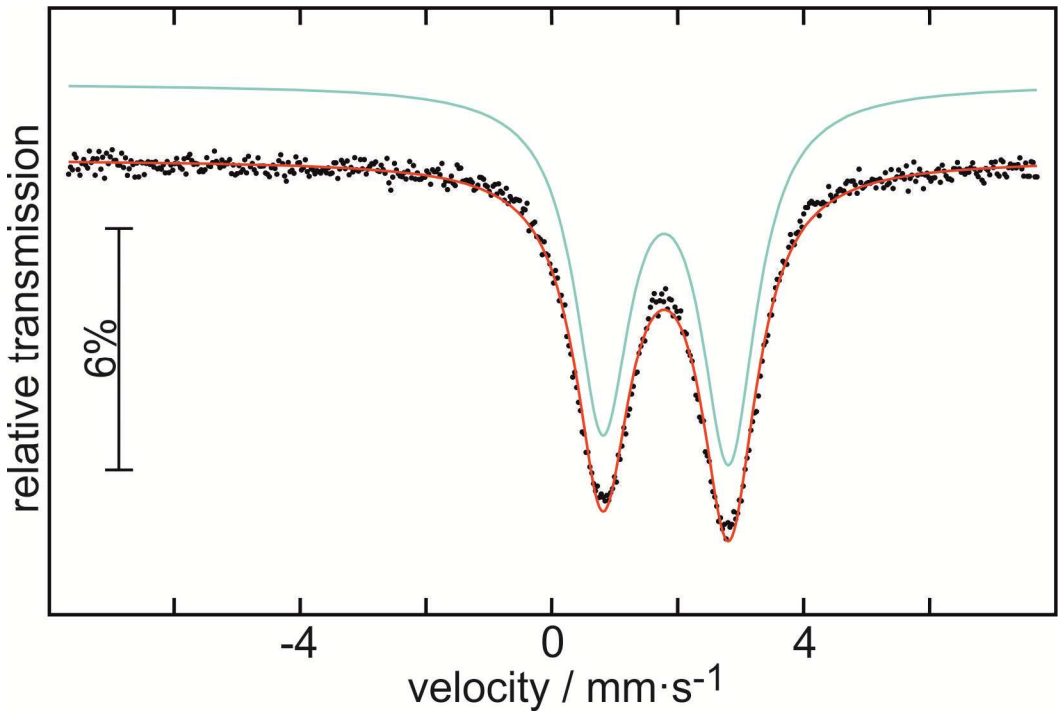

Figure SI2: ^{119}Sn Mössbauer spectrum of compound **3**·(THF). We expect the rather broad line width to arise from the disorder in the crystal structure of this compound. One of the dangling PyS ligands is disordered over two sites, thus the N atom of this ligand in its two alternative positions can coordinate the tin atom from a distance of 2.86 Å and 2.95 Å. Furthermore, the crystal structure contains solvent of crystallisation (THF), and partial loss of solvent during sample preparation might have contributed further to the enhanced line width.

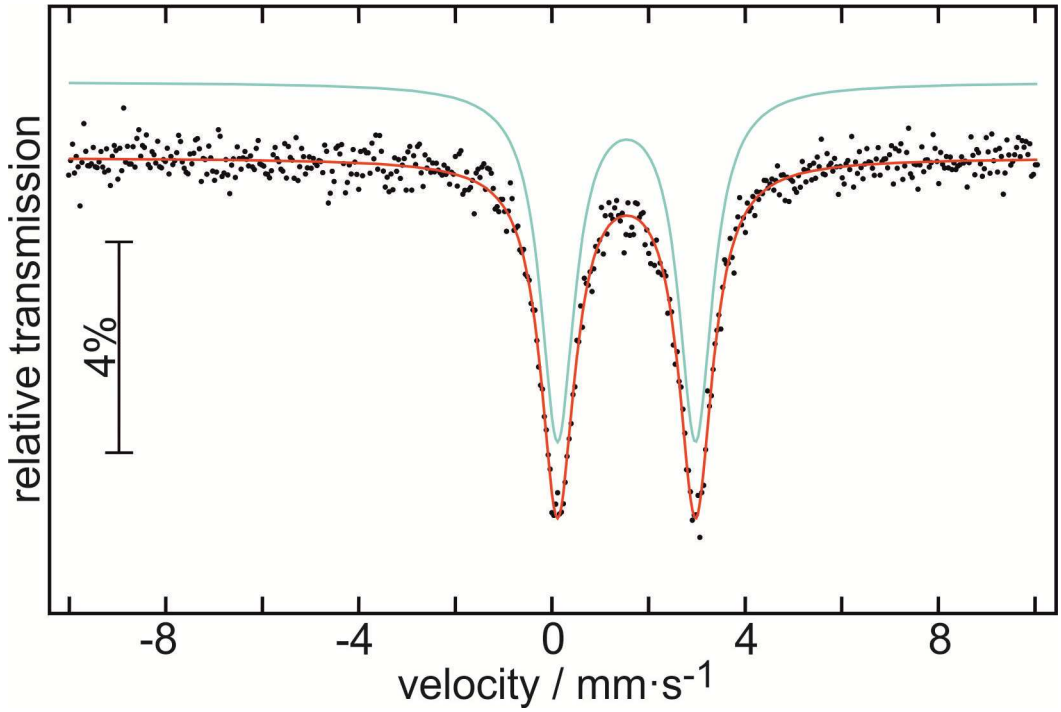

Figure SI3: ^{119}Sn Mössbauer spectrum of compound **4**.

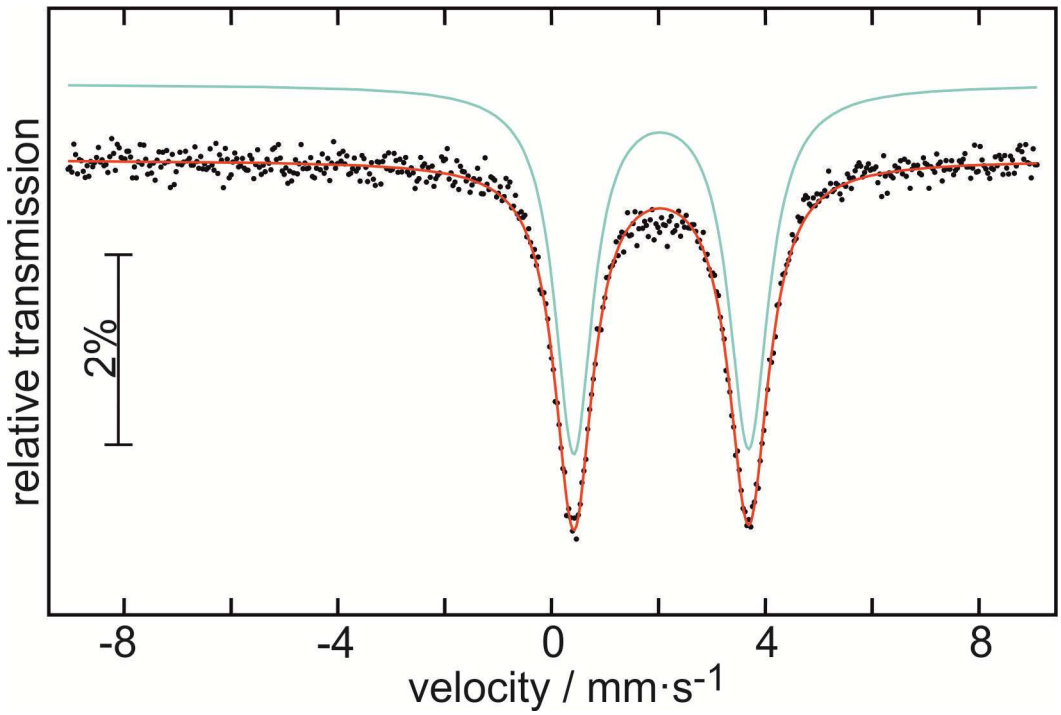

Figure SI4: ^{119}Sn Mössbauer spectrum of compound **5**·$(THF)_2$.

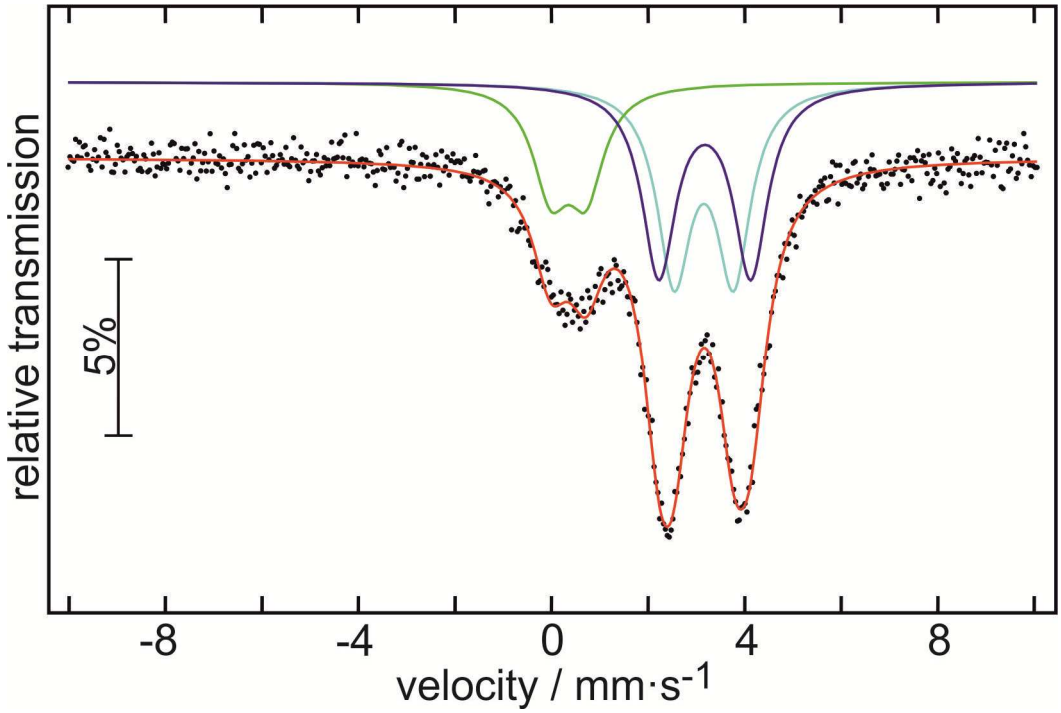

Figure SI5: ^{119}Sn Mössbauer spectrum of compound **III**. As shown by X-ray crystallography and ^{119}Sn solid state NMR spectroscopy[5] this solid contains two independent Sn sites in 1:1 ratio. This has been considered for the fitting of the Mössbauer spectrum. Furthermore, the sample (which was already aged) contained oxidation products (i.e., tin(IV) compounds).

Table SI2: Parameters of data collection and crystal structure refinement of compounds **1** (two modifications), **1·(CHCl$_3$)$_2$** and **4**.

	1 (modification a)	**1 (modification b)**	**1·(CHCl$_3$)$_2$**	**4**
Empirical formula	$C_{28}H_{23}Cl_2N_2PPdS_2Sn$	$C_{28}H_{23}Cl_2N_2PPdS_2Sn$	$C_{30}H_{25}Cl_8N_2PPdS_2Sn$	$C_{40}H_{33}N_2PPdS_2Sn$
Formula weight	778.56	778.56	1017.30	861.86
T (K)	200(2)	200(2)	200(2)	150(2)
λ (Å)	0.71073			
Crystal system	Triclinic	Triclinic	Monoclinic	Monoclinic
Space group	*P*-1	*P*-1	*C*2/*c*	$P2_1/c$
Unit cell dimens.				
a (Å)	8.7479(4)	11.9426(4)	36.1869(14)	16.3741(5)
b (Å)	11.8756(5)	11.9476(4)	10.7163(5)	9.4293(2)
c (Å)	15.2144(6)	12.0757(4)	22.1382(9)	23.7358(7)
α (°)	96.721(3)	82.183(3)	90	90
β (°)	93.528(3)	75.922(3)	119.940(3)	104.305(2)
γ (°)	107.858(3)	60.174(3)	90	90
V (Å^3)	1486.12(11)	1449.67(8)	7439.3(5)	3551.09(17)
Z / D_c (g/cm^3)	2 / 1.74	2 / 1.78	8 / 1.82	4 / 1.61
μ (mm^{-1})	1.8	1.9	1.9	1.4
F(000)	764	764	3984	1720
Crystal size (mm)	0.45×0.40×0.30	0.30×0.25×0.15	0.25×0.20×0.15	0.35×0.25×0.20
θ range (°)	2.46-32.00	1.74-32.00	2.01-32.00	1.91-32.00
Reflns collected	29645	32803	62249	47294
Unique reflns/R_{int}	10254 / 0.0178	10015 / 0.0602	12857 / 0.0415	12310 / 0.0531
Completeness to θ_{max}	99.4%	99.6%	99.7%	99.8%
Refinement	Full matrix least-squares on F^2			
Data / restraints / parameters	10254 / 0 / 334	10015 / 0 / 335	12857 / 30 / 426	12310 / 0 / 424
Goodness-of-fit on F^2	1.286	1.067	1.083	1.056
*R*1 / *wR*2 [I > 2σ(I)]	0.0235 / 0.0569	0.0343 / 0.0849	0.0321 / 0.0806	0.0294 / 0.0694
*R*1 / *wR*2 (all data)	0.0255 / 0.0575	0.0441 / 0.0894	0.0381 / 0.0834	0.0372 / 0.0720
Largest diff. peak and hole, eÅ^{-3}	0.485 / -0.699	1.041 / -1.293	0.796 / -1.111	0.909 / -1.203

Table SI3: Parameters of data collection and crystal structure refinement of compounds **3•(THF)**, **5•(THF)$_2$**, **2·(CHCl$_3$)$_2$** and **[Pd(PyS)$_2$(PPh$_3$)$_2$]**.

	3·(THF)	**5·(THF)$_2$**	**2·(CHCl$_3$)$_2$**	**[Pd(PyS)$_2$(PPh$_3$)$_2$]**
Empirical formula	$C_{42}H_{39}N_4OPPdS_4Sn$	$C_{64}H_{62}N_4O_2P_2Pd_2S_4Sn$	$C_{38}H_{32}Cl_{10}P_2PdSn$	$C_{46}H_{38}N_2P_2PdS_2$
Formula weight	1000.07	1440.85	1130.17	851.24
T (K)	150(2)	200(2)	200(2)	200(2)
λ (Å)				
Crystal system	Triclinic	Triclinic	Monoclinic	Monoclinic
Space group	*P*-1	*P*-1	$P2_1/n$	$P2_1/n$
Unit cell dimens.				
a (Å)	8.9822(3)	13.8400(6)	11.8853(2)	9.9959(8)
b (Å)	10.3340(4)	14.3813(6)	16.0997(2)	15.2833(11)
c (Å)	23.1347(8)	17.0641(7)	22.9151(4)	12.9857(10)
α (°)	100.226(3)	71.399(3)	90	90
β (°)	98.001(3)	75.459(3)	93.421(2)	97.233(7)
γ (°)	96.521(3)	72.174(3)	90	90
V (Å^3)	2071.55(13)	3019.8(2)	4376.99(12)	1968.0(3)
Z / D_c (g/cm^3)	2 / 1.60	2 / 1.59	8 / 1.72	2 / 1.44
μ (mm^{-1})	1.3	1.2	1.7	0.7
F(000)	1004	1452	2224	872
Crystal size (mm)	0.17×0.15×0.05	0.30×0.22×0.08	0.40×0.30×0.20	0.40×0.30×0.25
θ range (°)	2.44-30.00	2.46-30.00	1.55-30.00	2.43-27.00
Reflns collected	64024	44439	79190	18390
Unique reflns/R_{int}	12068 / 0.0593	17590 / 0.0310	12735 / 0.0298	4298 / 0.0756
Completeness to θ_{max}	99.8%	99.9%	99.7%	99.8%
Refinement				
Data / restraints / parameters	12068 / 10 / 513	17590 / 51 / 730	12735 / 12 / 508	4298 / 0 / 241
Goodness-of-fit on F^2	1.149	1.029	1.160	1.049
$R1$ / $wR2$ [I > 2σ(I)]	0.0261 / 0.0562	0.0280 / 0.0669	0.0286 / 0.0692	0.0380 / 0.0676
$R1$ / $wR2$ (all data)	0.0323 / 0.0580	0.0375 / 0.0705	0.0321 / 0.0707	0.0744 / 0.0770
Largest diff. peak and hole, eÅ^{-3}	0.539 / -0.653	0.731 / -0.668	0.536 / -0.692	0.613 / -1.075

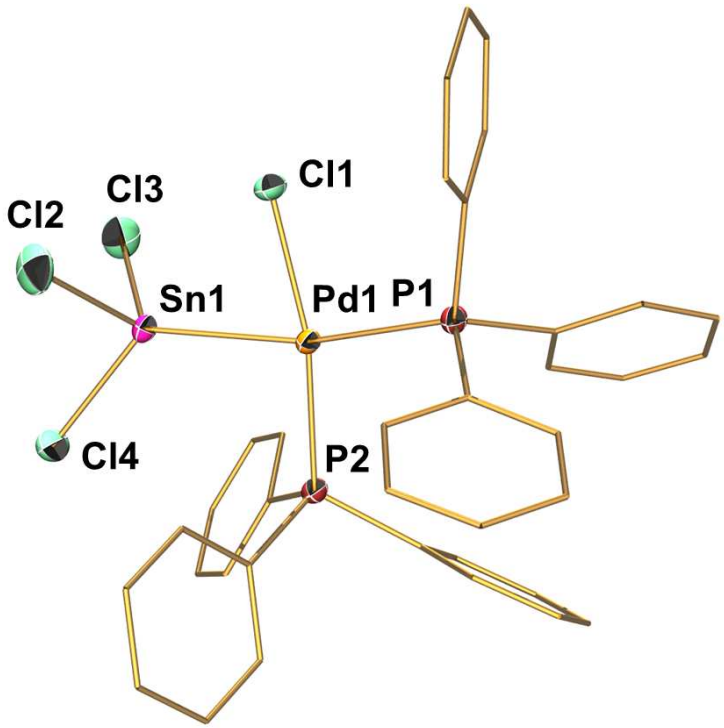

Figure SI6: Molecular structure of compound **2** in the crystal structure of **2·(CHCl$_3$)$_2$**. Selected atoms are labelled, displacement ellipsoids show 50% probability, for clarity H atoms are omitted and PPh_3 groups are simplified as stick model.

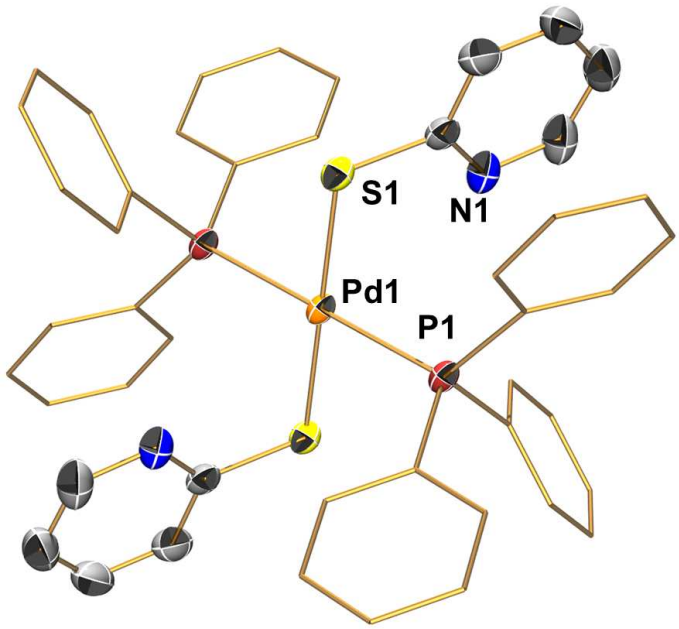

Figure SI7: Molecular structure of [Pd(PyS)$_2$(PPh$_3$)$_2$] in the crystal. Selected atoms are labelled, displacement ellipsoids show 50% probability, for clarity H atoms are omitted and PPh_3 groups are simplified as stick model. The Pd atom is located on a centre of inversion, thus the asymmetric unit consists of ½ molecule.

The structures of **1**, **3, 4** and **5** have been partly optimised at PBE[9] level of theory as implemented in ADF.[10] The X-ray coordinates of the atoms (from **1** (modification a, see Table SI2), **3**·(THF), **4** and **5**·$(THF)_2$, respectively) have been kept constant while the hydrogen atoms have been relaxed. The optimisations have been carried out using scalar relativistic corrections,[11] applying Triple-Zeta polarised (TZP) basis set for the elements of the first and second row of the periodic table, and Triple-Zeta double polarised (TZ2P) basis set for the heavier elements.[12] (The Electron Localization Function, Figures SI9 and SI10, is visualised from the electron densities computed with ADF package at the level described above.)
NBO analysis[13] has been carried out with Gaussian software package[14] for the partly optimised molecular structures of **1**, **3, 4** and **5** (see below). The PBE[9] Functional and DZVP basis set[15] have been applied to obtain the natural charges of the system. Gauss view 5.0 (from the Gaussian visualization package) was used to generate the diagrams shown in Figure SI8.

Table SI4: Natural charges (NC) and valence shell electron configurations for Sn and Pd calculated for compounds **1**, **3**, **4** and **5**.

	NC(Sn)	NC(Pd)	Sn		Pd
			configuration	s/p ratio	configuration
1	1.75	-0.60	5s(1.05) 5p(1.18) 5d(0.03) 6p(0.01)	0.89	5s(0.42) 4d(9.36) 5p(0.81) 5d(0.02)
3	1.67	-0.61	5s(1.11) 5p(1.18) 6s(0.01) 5d(0.02) 6p(0.03)	0.94	5s(0.38) 4d(9.37) 5p(0.85) 5d(0.02)
4	1.82	-0.57	5s(0.94) 5p(1.23) 6s(0.01) 5d(0.01) 6p(0.02)	0.76	5s(0.40) 4d(9.37) 5p(0.79) 5d(0.02)
5	1.80	-0.71	5s(1.09) 5p(1.10) 5d(0.01) 6p(0.02)	0.99	5s(0.40) 4d(9.41) 5p(0.88) 6s(0.01) 5d(0.02) 5s(0.40) 4d(9.41) 5p(0.89) 6s(0.01) 5d(0.02)

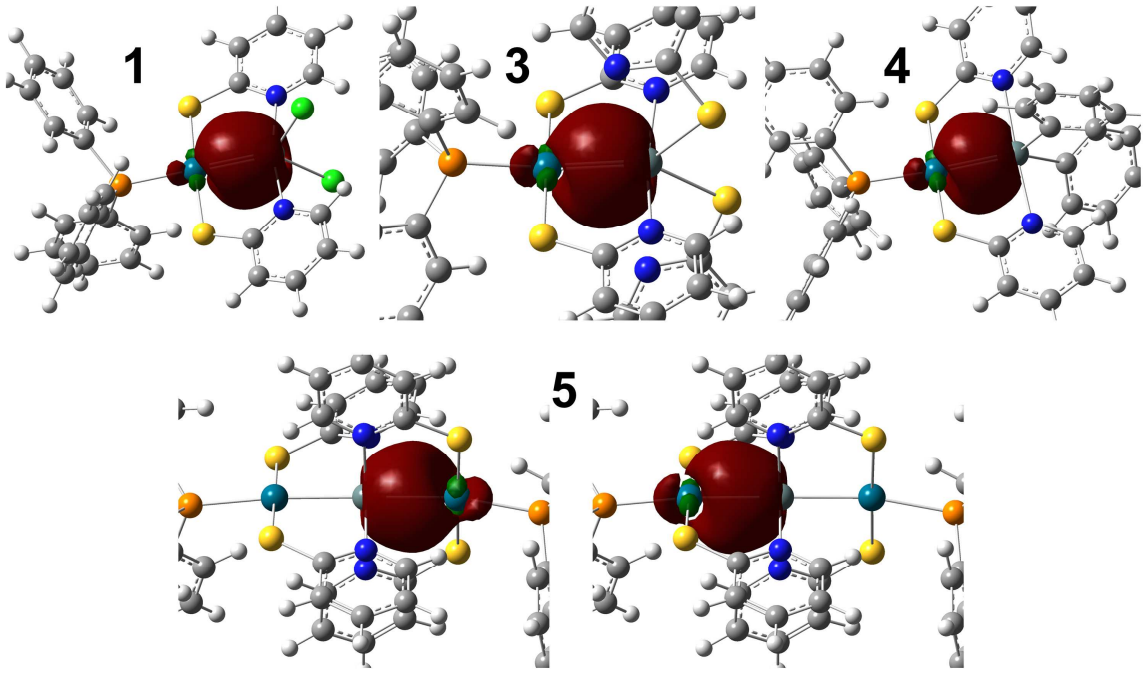

Figure SI8: NBOs of the Pd–Sn bonds in **1**, **3**, **4** and **5** depicted with a contour value of 0.05.

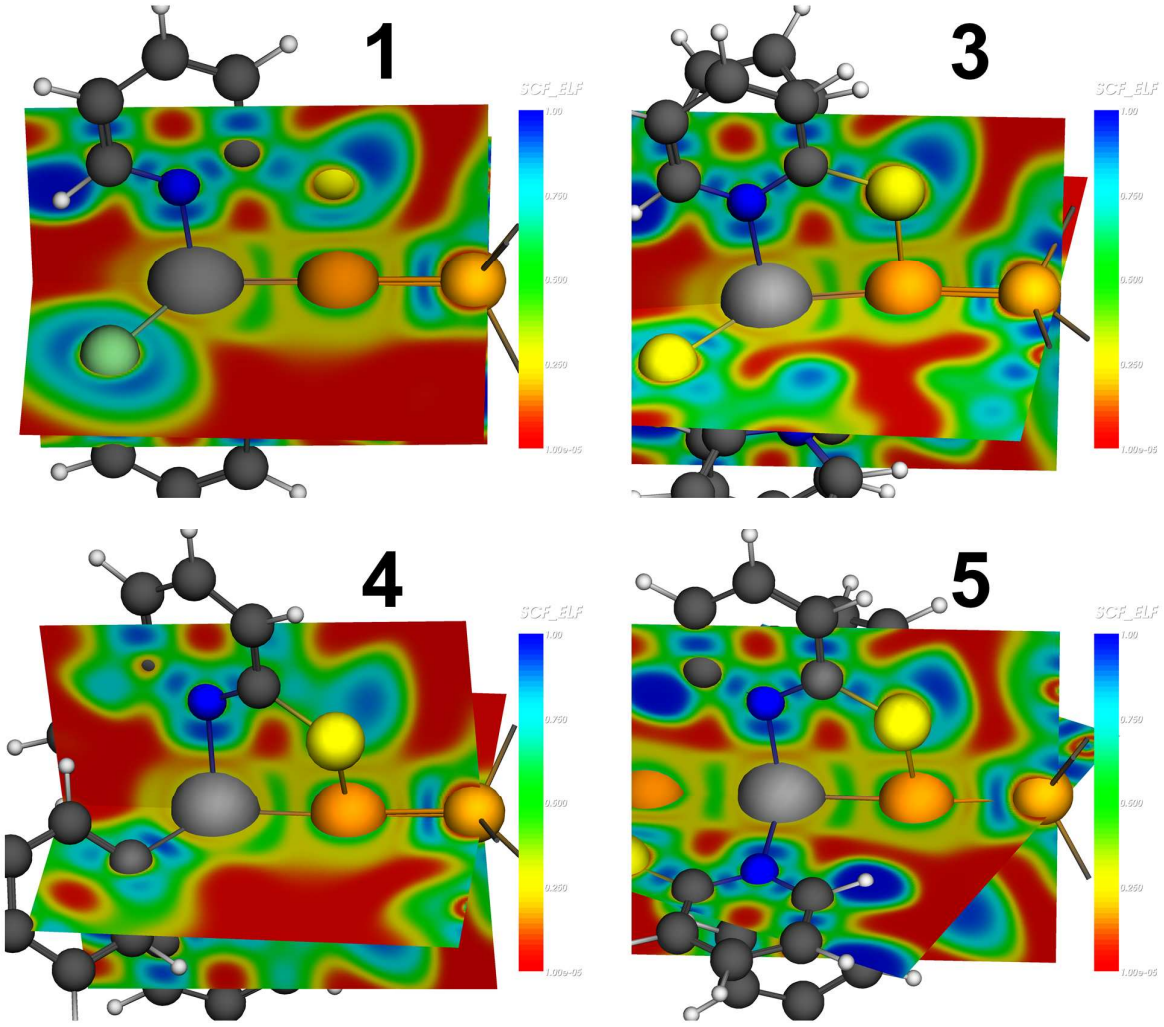

Figure SI9: Electron Localization Function (ELF) around the Pd–Sn bonds in **1**, **3**, **4** and **5** depicted with a linear scale (red = 0.00, green = 0.50, blue = 1.00). The ELF representations consist of two planes each, which intersect in the Pd–Sn bond. One of the planes contains the Pd and Sn atom as well as a pyridine-2-thiolato N atom, the other plane contains the Pd and Sn atom as well as the Sn–X bond to one of the monodentate substituents (**1**, **3**, **4**) or to another pyridine N atom (**5**).

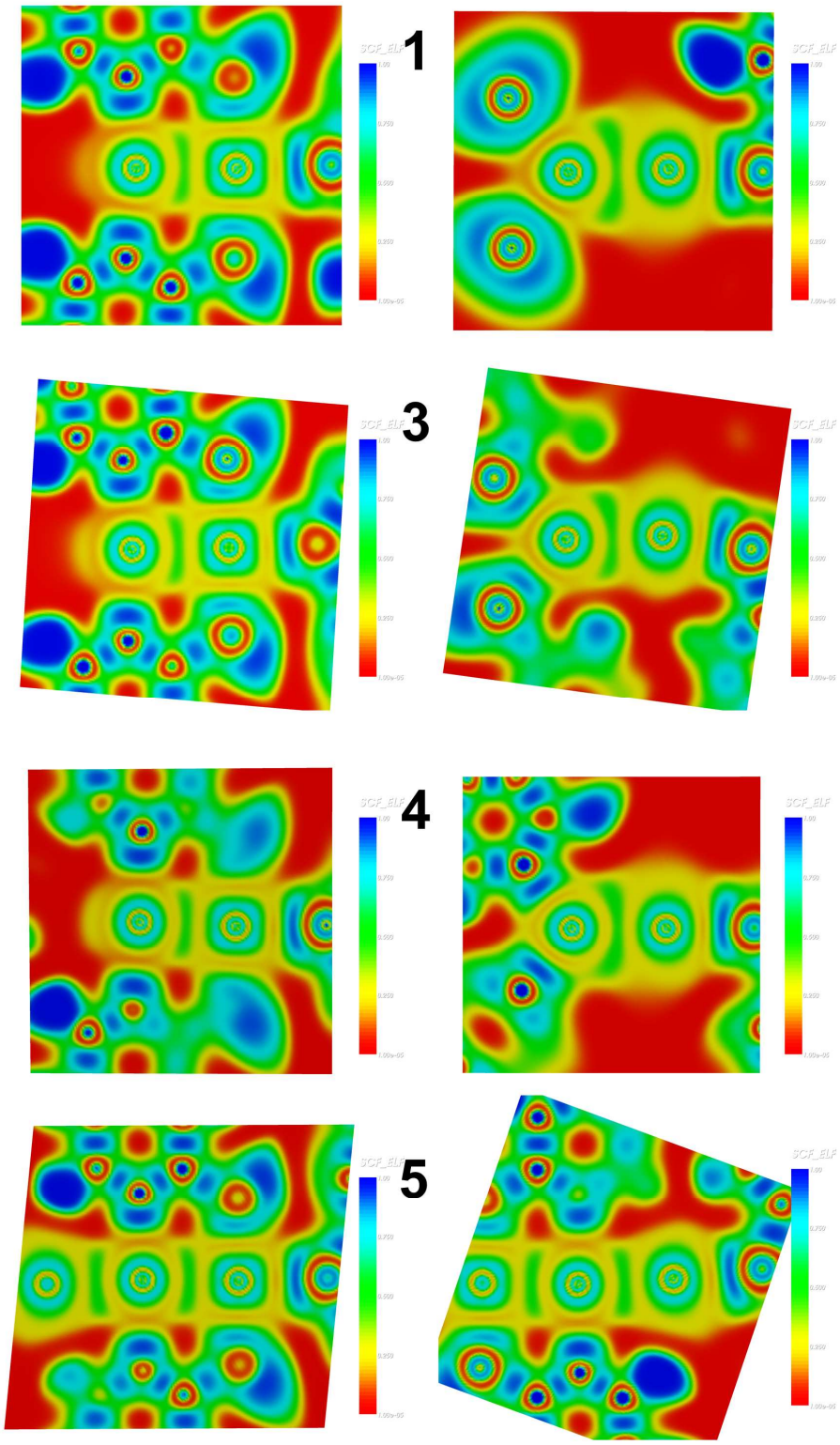

Figure SI10: Electron Localization Function (ELF) around the Pd–Sn bonds in **1**, **3**, **4** and **5** depicted with a linear scale (red = 0.00, green = 0.50, blue = 1.00). These 2D diagrams were used to create Figure SI9. Each of the planes in the left column contains the Pd and Sn atom as well as a pyridine-2-thiolato N atom, the corresponding plane in the right column contains the Pd and Sn atom as well as the Sn–X bond to one of the monodentate substituents (**1**, **3**, **4**) or to another pyridine N atom (**5**).

[1] E. Wächtler, R. Gericke, S. Kutter, E. Brendler, J. Wagler, *Main Group Met. Chem.*, **2013**, in production, doi: 10.1515/mgmc-2013-0041.
[2] M. Masaki, S. Matsunami, *Bul. Chem. Soc. Jap.* **1976**, *49*, 3274–3279.
[3] M. Bouâlam, J. Meunier-Piret, M. Biesemans, R. Willem, M. Gielen, *Inorg. Chim. Acta* **1992**, *198–200*, 249–255.
[4] Y. Nakatsu, Y. Nakamura, K. Matsumoto, S. Ooi, *Inorg. Chim. Acta* **1992**, *196*, 81–88.
[5] J. S. Morrison, H. M. Haendler, *J. Inorg. Nucl. Chem.* **1967**, *29*, 393–400.
[6] R. A. Michelin, L. Zanotto, D. Braga, P. Sabatino, R. J. Angelici, *Inorg. Chem.* **1988**, *27*, 85–92.
[7] G. M. Sheldrick, *Acta Crystallogr. A* **2008**, *64*, 112-122.
[8] R. A. Brand, *Normos Mössbauer fitting Program* (Universität Duisburg) **2002**.
[9] J.P. Perdew, K. Burke, M. Ernzerhof, *Phys. Rev. Lett.* **1996**, *77*, 3865-3868.
[10] ADF2012.01: J. Autschbach, D. Bashford, A. Brces, F.M. Bickelhaupt, C. Bo, P.M. Boerrigter, L. Cavallo, D.P. Chong, L. Deng, R.M. Dickson, D.E. Ellis, M. van Faassen, L. Fan, T.H. Fischer, C. Fonseca Guerra, A. Ghysels, A. Giammona, S.J.A. van Gisbergen, A.W. Götz, J.A. Groeneveld, O.V. Gritsenko, M. Grüning, S. Gusarov, F.E. Harris, P. van den Hoek, C.R. Jacob, H. Jacobsen, L. Jensen, J.W. Kaminski, G. van Kessel, F. Kootstra, A. Kovalenko, M.V. Krykunov, E. van Lenthe, D.A. McCormack, A. Michalak, M. Mitoraj, J. Neugebauer, V.P. Nicu, L. Noodleman, V.P. Osinga, S. Patchkovskii, P.H.T. Philipsen, D. Post, C.C. Pye, W. Ravenek, J.I. Rodrguez, P. Ros, P.R.T. Schipper, G. Schreckenbach, J.S. Seldenthuis, M. Seth, J.G. Snijders, M. Sol, M. Swart, D. Swerhone, G. te Velde, P. Vernooijs, L. Versluis, L. Visscher, O. Visser, F. Wang, T.A. Wesolowski, E.M. van Wezenbeek, G. Wiesenekker, S.K. Wolff, T.K. Woo, A.L. Yakovlev, E.J. Baerends, T. Ziegler. Adf2012, scm, theoretical chemistry, Vrije Universiteit, Amsterdam, the Netherlands, http://www.scm.com. ADF2012, SCM.
ADF2010.01: C. Fonseca Guerra, J.G. Snijders, G. te Velde, E.J. Baerends, *Theor. Chem. Acc.* **1998**, *99*, 391-403; G. te Velde, F.M. Bickelhaupt, E.J. Baerends, C. Fonseca Guerra, S.J.A. van Gisbergen, J.G. Snijders, T. Ziegler, *J. Comput. Chem.* **2001**, *22*, 931-967; http://scm.com
[11] E. van Lenthe, E.J. Baerends, J.G. Snijders, *J. Chem. Phys.* **1993**, *99*, 4597-4610.
[12] E. van Lenthe, E. J. Baerends. Optimized slater-type basis sets for the elements 1-118. *J. Comput. Chem.* **2003**, *24*, 1142-1156.
[13] a) Gaussian NBO Version 3.1; b) J. P. Foster and F. Weinhold, Natural hybrid orbitals J. Am. Chem. Soc. 102, 7211 (1980); b) Reed, A. E. And Weinhold, F. Natural Bond Orbital Analysis Of Near-Hartree-Fock Water Dimer Journal Of Chemical Physics, 78, 4066 (1983); c) Reed, A. E. And Weinstock, R. B. And Weinhold, F. Natural-Population Analysis Journal Of Chemical Physics, 83, 735 (1985); d) Reed, A. E. And Weinhold, F. Natural Localized Molecular-Orbitals Journal Of Chemical Physics, 83, 1736 (1985).

[14] Gaussian 03, Revision E.01, M. J. Frisch, G. W. Trucks, H. B. Schlegel, G. E. Scuseria, M. A. Robb, J. R. Cheeseman, J. A. Montgomery, Jr., T. Vreven, K. N. Kudin, J. C. Burant, J. M. Millam, S. S. Iyengar, J. Tomasi, V. Barone, B. Mennucci, M. Cossi, G. Scalmani, N. Rega, G. A. Petersson, H. Nakatsuji, M. Hada, M. Ehara, K. Toyota, R. Fukuda, J. Hasegawa, M. Ishida, T. Nakajima, Y. Honda, O. Kitao, H. Nakai, M. Klene, X. Li, J. E. Knox, H. P. Hratchian, J. B. Cross, V. Bakken, C. Adamo, J. Jaramillo, R. Gomperts, R. E. Stratmann, O. Yazyev, A. J. Austin, R. Cammi, C. Pomelli, J. W. Ochterski, P. Y. Ayala, K. Morokuma, G. A. Voth, P. Salvador, J. J. Dannenberg, V. G. Zakrzewski, S. Dapprich, A. D. Daniels, M. C. Strain, O. Farkas, D. K. Malick, A. D. Rabuck, K. Raghavachari, J. B. Foresman, J. V. Ortiz, Q. Cui, A. G. Baboul, S. Clifford, J. Cioslowski, B. B. Stefanov, G. Liu, A. Liashenko, P. Piskorz, I. Komaromi, R. L. Martin, D. J. Fox, T. Keith, M. A. Al-Laham, C. Y. Peng, A. Nanayakkara, M. Challacombe, P. M. W. Gill, B. Johnson, W. Chen, M. W. Wong, C. Gonzalez, and J. A. Pople, Gaussian, Inc., Wallingford CT, 2004.

[15] N. Godbout, D. R. Salahub, J. Andzelm, and E. Wimmer, Optimization of Gaussian-type basis sets for local spin density functional calculations. Part I. Boron through neon, optimization technique and validation. Can. J. Chem. 70, 560 (1992).